An Experimental Analysis of Tyndall Figures

NERC Research Experience Placement

Summer 2013

Author:
Peter Harvey

Supervisors:
Dr. Richard F. Katz
Matthew Hennessy

Contents

Chapter 1

Introduction

Tyndall figures were first discovered by John Tyndall in 1857 [17]. He focussed sunlight onto a sample of glacial ice and observed internal melting through a magnifying glass. The melt figures that he observed were 'flowers' forming inside the sample of ice, all of which were orientated in the same way. We now know that Tyndall figures are internal melt figures that always form in the basal plane of ice crystals, usually due to the absorption of visible/infrared light. Tyndall figures generally exhibit a six-fold symmetry in the basal plane and are often referred to as 'Tyndall flowers', 'Tyndall stars' or 'Inverse snowflakes'. A vapour bubble (cavitation bubble) is always present in Tyndall figures, caused because water is more dense than ice.

In the 3d plane, Tyndall figures have an interesting profile. A symmetric parabola is often assumed in theoretical studies [9] however Tyndall figures have been observed to have a bevelled edge which is at its thickest at the centre (where the cavitation bubble is formed) and that tails off to a minimum at the water-ice interface.

Work has been done to model the growth of Tyndall figures [4] and experimental evidence is required to help build up a full picture of the formation and growth of Tyndall figures.

The aims for summer 2013 were to:

1. Create an illumination system that uses very intense visible light from a halogen bulb (or similar).
2. Check that this light source does indeed produce Tyndall figures.
3. Develop observational technique to generate time-series photographs allowing for quantitative measurement of the characteristics of the figures.
4. Quantify the light source in terms of intensity and spectrum.

This document will explore the techniques used in the pursuit of these goals.

Chapter 2

Physical Processes Underlying Tyndall Figures

Here I will try to provide a rough-and-ready overview of some of the main physical processes underlying the formation and growth of Tyndall figures. Everything here has been explained far more comprehensively by others; this section is to give an overview of the processes and the implications on the morphology of Tyndall figures. Most of the processes are very well explained by Hennessy [4] and it is worth following up on the references in Chapter 2 of his thesis as they contain rigorous derivations of the formulae in this section. Ice Physics [6] is also a good starting point for understanding the processes at work.

2.1 Nucleation

Tyndall figures nucleate at imperfections in the crystal lattice. There is evidence that these imperfections could be caused by submicroscopic gaseous inclusions [11] or other colloidal particles [12]. There is also evidence that imperfections in the crystal lattice caused by interaction with a high energy neutron nucleate Tyndall figures [3].

Regardless of what causes the imperfection in the lattice, the mechanism for nucleation is the same. It is possible to superheat pure crystals of ice above 0°C without nucleating melting. It is proposed that nucleation of Tyndall figures occurs when the lattice is superheated by a few tenths of a degree [10]. At imperfections, the intermolecular forces between the water molecules in the ice are weakened and melting is nucleated.

2.2 Growth

The main physical principle that governs the evolution of a solid and liquid phase is that of conservation of thermal energy. A statement of this can be written as:

$$\frac{\partial}{\partial t}(\rho_i c_{pi} T_i) + \nabla \cdot \mathbf{J}_i = Q_i \tag{2.1}$$

Where ρ_i, c_{pi} and T_i denote the density, specific heat capacity and temperature of a phase i. $\mathbf{J}_i$ is the thermal flux through the phase and Q_i represents a source of heat.

The main contribution to thermal flux across the solid an liquid phase in this case is from diffusion. Diffusion arises from the tendency of heat to flow from high temperature regions to lower temperature regions. This can be quantified using Fourier's law of heat conduction:

$$\mathbf{J}_d = -k_i \nabla T_i \tag{2.2}$$

Where k_1 is the thermal conductivity of a phase.

The heat source in this case is a halogen light bulb. The intensity of a beam of light decays exponentially with distance travelled. The volumetric heating caused by a beam is equal to the power lost by that beam as it travels through a medium. This can be quantified as:

$$Q_i = \alpha_i I_0 e^{-\alpha_s z} \tag{2.3}$$

It is important to note that water absorbs light and infrared radiation almost 100 times better than ice does.

The conditions at the water-ice interface have the largest implications for the morphology of Tyndall figures. If the temperature across the interface is equal, $T_I = T_s = T_l$, then the temperature can be calculated from the Gibbs-Thomson condition, which establishes the equilibrium melting temperature for a curved interface. This is well explained by Hennessy [4], so here I will just state the equation and discuss its consequences. The Gibbs-Thomson condition:

$$T_I = T_m \left(1 - \kappa \frac{\gamma}{\rho L}\right) \tag{2.4}$$

Where T_I is the interfacial temperature, T_m is equilibrium temperature, κ is a measure of the curvature of the interface and γ is the surface energy. ρ and L are density and latent heat of fusion. The shape of a Tyndall Figure is the result of a highly curved interface between solid and liquid phases. Intermolecular forces at the interface lead to a surface energy, which nature tries to minimise. The mechanism for reducing surface energy is a shift in phase equilibria that causes heat to diffuse from liquid fingers to solid fingers. Liquid fingers freeze and solid fingers melt, minimising surface area. The curvature of a liquid finger extending into a solid

is taken as negative. If the curvature is zero, the interface is a straight line and $T_m = T_I$. Superheating in the solid phase leads to instability in the interface, superheating in the liquid phase promotes stability in the interface.

Well defined geometries in the crystal lattice give rise to anisotropies in the surface energy.Ice has a hexagonal structure and Tyndall figures show strong six-fold symmetry - this implies effects of surface energy anisotropy (microscopic properties) are propagated to the macro scale. Thus the expression for the Gibbs Thomson condition needs to be edited to include the effects of surface energy anisotropy. It can be written as:

$$T_I = T_M \left(1 - \kappa \frac{\gamma + \gamma_{\theta\theta}}{\rho L}\right) \tag{2.5}$$

Where the θ subscript denotes differentiation with respect to theta. A new expression for the surface energy is defined as:

$$\gamma = \gamma_0 \left[1 + \frac{\sigma_n}{n^2 - 1} cos(n\theta)\right] \tag{2.6}$$

Where σ_n is a measure of the anisotropy. When $\sigma_n > 1$, the anisotropy is weak and the expression $\gamma + \gamma_{\theta\theta}$ will have the same sign for all θ. Strong anisotropy occurs when $\sigma_n < 1$. When in equilibrium, $\kappa(\gamma + \gamma_{\theta\theta})$ is constant. This leads to the interface looking approximately circular when the anisotropy is weak. When the anisotropy is strong, the interface will look more corrugated.

The stefan condition gives an expression for the velocity (v_n) of the interface:

$$(\rho L + \gamma\kappa)v_n = -k_l \nabla T_l \cdot \mathbf{n} + k_s \nabla T_s \cdot \mathbf{n} \tag{2.7}$$

This expression essentially states that the interface will grow quickly if there is superheating in the solid. This explains the dendritic growth of Tyndall figures irradiated with higher power light - as the light superheats the ice, the interface must grow quickly to try to minimise the surface tension. The size of the interface is greatly increased with dendritic growth, compared with discoid growth.

Chapter 3

Methodology

In this section I will provide a detailed explanation of the systems and methods used in the analysis of Tyndall figures. Firstly, I will outline the methods for producing optically perfect crystals of ice. I will then go through the apparatus used to produce, image and measure Tyndall figures, explaining the importance of each component and the reasoning behind the experimental set-up.

3.1 Production of Large, Optically Perfect Crystals of Ice

Putting in place a process to consistently produce large crystals of ice with a known crystallographic orientation is the basis of any experimental investigation into Tyndall figures. Much of the previous research into Tyndall figures has been undertaken at institutions conveniently close to glaciers, which are an excellent source of large single crystals of ice. Unfortunately the countryside of Oxfordshire is devoid of glaciers, so samples of ice must be grown in the lab. Many standard techniques have been well documented [5, 13] but these techniques are somewhat complex in comparison to the method outlined here. This process is a simplified version of the technique outlined by Knight [7]. This process will produce large crystals of ice that are optically perfect to naked-eye inspection and inspection using crossed polarisers.

The technique involves two stages: growing a seed crystal and then producing the ice single crystal for use in experiments. Both of these stages require the use of a refrigerator with a temperature controller.

The controller used is a Tempatron IR32 Temperature and Process Controller. Hysteresis is used to control the temperature. The controller will turn the refrigerator on when the temperature is above a certain point and will not switch it off until the temperature falls below another given point. In this case, the hysteresis is set to 0.3, meaning that the refrigeration will switch on when the measured temperature is 0.3°C above the desired temperature and then switch it off when the measured temperature is 0.3°C below. This means that the temperature of the fridge will oscillate around the inputted temperature.

During the ice forming process, the desired temperature is -3°C. The controller should be

programmed for this temperature. To change the programmed temperature, push 'SEL' and hold it down for 5 seconds. Upon release, the display will begin to flash with the current programmed temperature. Adjust this to the desired temperature using the arrow buttons and confirm the new temperature by pressing 'SEL' once.

It should be noted that the temperature inside the refrigerator is in-homogenous. Figure 3.1 is a labelled diagram of the fridge. It is found that sections labeled A and B are marginally cooler than section C. There is also a temperature gradient horizontally; section C_1 is warmer than section C_3 and the front of the fridge is warmer than the back of the fridge. The implications of this will be discussed as they arise.

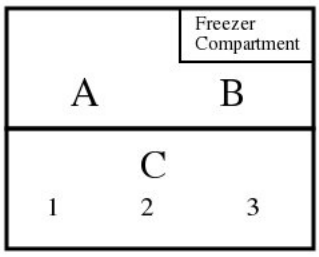

Figure 3.1: (Simplified) Diagram of the Fridge Interior.

3.1.1 Growing The Seed

A suitable crystal for seeding growth of ice single crystals must have it's c-axis orientated perpendicular to the surface of the water it is grown on. This is to ensure the orientation of the c-axis of the ice single crystal is known. The seed itself must also be an ice single crystal. It is found that dendrites that grow on the surface of slightly supercooled water make for very good seeds [13].

In order to grow these dendrites, a large tupperware container (19cm x 12 cm x 4cm) is filled two thirds full with distilled water, placed in foam insulation, and covered. This container is then placed in section A of the fridge (see figure 3.1). It is suspected that nucleation of ice is caused by tiny frost particles that become dislodged from the refrigeration unit and settle on the surface of the water. To prevent multiple nucleations, the container is covered whilst cooling. Once the fridge temperature reads -2°C, the covering is removed from the container and replaced by a covering with a 1cm x 1cm hole cut in it. This is to allow a frost particle to fall from the freezer compartment and settle on the surface. This frost particle will nucleate the growth of a dendrite on the surface. The dendrite that grows will be a suitable seed when it is around 1cm x 1cm in size.

3.1.2 Producing The Single Crystal

A tupperware container (dimensions 12cm x 9cm x 4cm) is placed in a surround of approximately 4cm of foam insulation and this container is filled with 225ml of de-ionised water that has been refrigerated to below 1°C. The seed crystal is then carefully floated on the surface of the water. The water does not need to be supercooled, just cold enough to prevent the seed from melting on contact. The container is covered and placed into the refrigerator. Three containers will fit in section C of the fridge, one in each of C_1, C_2 and C_3 respectively (see figure 3.1).

As previously mentioned, C_1 is warmer than C_3 and the front of the fridge is warmer than the back of the fridge. This can lead to ice single crystals that are wedge shaped (where the colder region has caused ice to grow faster). This problem can be overcome by carefully rotating the tupperware half way through the forming process. All tupperware should be rotated 180°and the tupperware in sections C_1 and C_3 should be swapped over to negate the fact that C_1 is warmer than C_3.

3.1.3 A Note on Timings

With the fridge set to maintain a temperature of -3°C, the above process should take 7 hours on average. It is advantageous to have refrigerated the distilled water to a temperature of 0°C so that you can immediately begin producing a seed crystal first thing in the morning. With pre-cooled water, it takes 40 minutes to grow a suitable seed crystal.

The tupperware that you use to grow the ice single crystals should be kept at room temperature and filled with cooled water when the seed crystal is ready. This is because the tupperware provides a good nucleation point for ice when cooled. Sometimes ice growth will nucleate from the walls of the tupperware and you will get a sample that is an aggregate of many small crystals of ice and useless for experimentation.

The time between seeding the water in C_1, C_2 and C_3 and rotating the containers is around 3 hours, meaning that the entire process for growing 10mm thick ice single crystals takes about 6 hours.

If the ice single crystals are seeded at 10:00 in the morning, they should be ready for experimentation by around 16:00 the same day.

3.1.4 Imperfections

If a crystal of ice is optically “perfect” then it has no visible imperfections. The transparency of a single crystal of ice is quite astounding. On inspection through two crossed polarisers, each crystal of ice will appear a slightly different colour. This is because crystals of ice are birefringent, meaning that the refractive index depends on polarisation and direction of propagation of light. A sample usable for producing Tyndall figures should be composed of two or three large crystals and appear optically “perfect”.

On inspection, a sample of ice may appear optically perfect. However, this does not mean that the crystal lattice is completely free of microscopic imperfections. It is from these imperfections that Tyndall figures nucleate. In my experience, even the milli-Q water (the highest purity water available in the department) produced ice with microscopic imperfections. Ideally only a single Tyndall figure would be nucleated per test, so there is a balancing act between having enough imperfections to produce Tyndall figures and having few enough to produce a sensible number of figures per test.

If Tyndall figures do not appear to nucleate, it is often worth producing some samples of ice 'doped' with salt (or another soluble substance). These samples of ice should be full of imperfections, so that many Tyndall figures will be nucleated. This will determine whether the apparatus you are using is capable of producing Tyndall figures.

3.2 Light Source

As discussed in his report, Tyndall produced Tyndall figures by focussing sunlight onto crystals of glacial ice. Obviously, sunlight is not a practical light source to use in a lab, so another source is required.

I explored three options for a light source:

1. A calibrated halogen light source with variable brightness / intensity
2. A more commercially available halogen light source (overhead projector, slide projector, etc.)
3. An infrared laser

On first consideration, a laser appears to be the perfect light source for producing Tyndall figures. It is coherent and monochromatic, meaning that intensity and absorption coefficients can be easily obtained. Extensive investigations using a $500mW$ infrared laser were undertaken by Michael Fergusson in Sumer 2012. Interestingly, the laser did not produce Tyndall figures. The reason for this is still not known. It could be that because the laser only has a small spot size, the likelihood of the beam being incident on an imperfection is low. It could be that the power is too high or too low - internal melting is sometimes observed with the laser, but the figures never go unstable (in fact, they behave somewhat differently to Tyndall figures). It could also be that the wavelength of light produced by the laser was somehow 'wrong', but this is unlikely as the laser is a frequency which is well absorbed by ice. Regardless of the reason for the laser not working, I decided to begin with a light source that would definitely produce Tyndall figures, so the laser was not an option. This left a halogen light source. In the end, I decided to purchase a slide projector. A laboratory calibrated light source would have been considerably more expensive and would have been equally difficult to quantify. All halogen bulbs are designed to operate at a colour temperature of around 3000K so they all have very similar intensity profiles (figure 3.2 shows examples of intensity profiles for a selection of halogen lamps [18]).

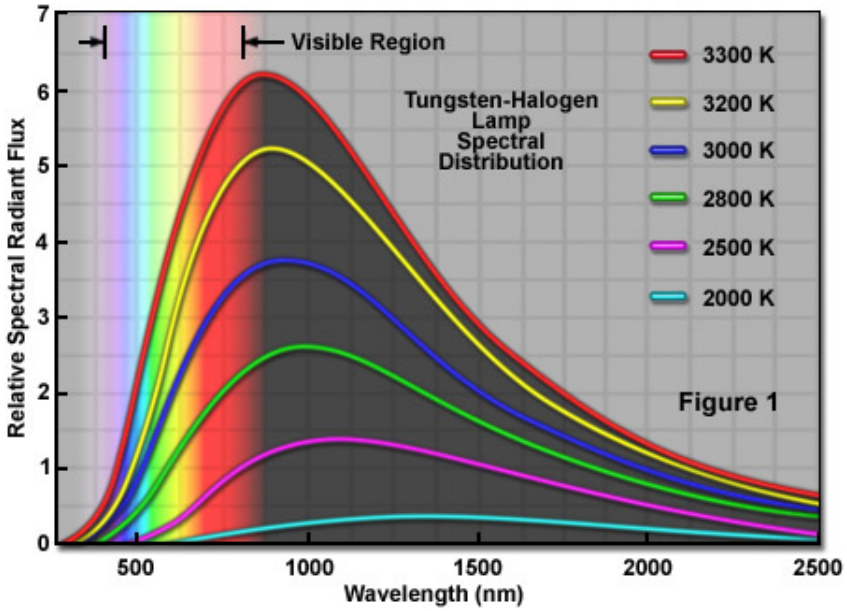

Figure 3.2: A graph to show how the intensity profile of halogen bulbs change with colour temperature.

The slide projector that I used was a Voigtlander VP135AF with a 150W 24V halogen bulb. Using a power meter I measured how the power changed with distance from the bulb, the results are shown in graph 3.3.

The slide projector appeared to have a lens to collimate the light. A brief test for collimation is to hold a piece of paper in front of the source, note down the beam's size and shape (in this case it is circular), and then slowly move the paper away from the source. If collimated, the shape and size of the beam should be relatively constant. It turns out that this is not the case for the slide projector, where the beam was found to spread out significantly. The beam cannot be treated as collimated in any calculations.

3.3 Beam Manipulation

The slide projector proved to be highly effective in producing Tyndall figures, but because it has no in-built method of varying the intensity, an external system of filters was required to manipulate the beam of light. Changing the characteristics of the beam provides insight into how the morphology of the figures changes with intensity. The amount of time that the ice is subject to room-temperature surroundings should be minimised to ensure that the light is the main source of superheating in the crystal. Using filters to vary the intensity is much faster than changing the ice-source distance between experiments. This means that multiple measurements with varying intensity can be taken from one ice sample.

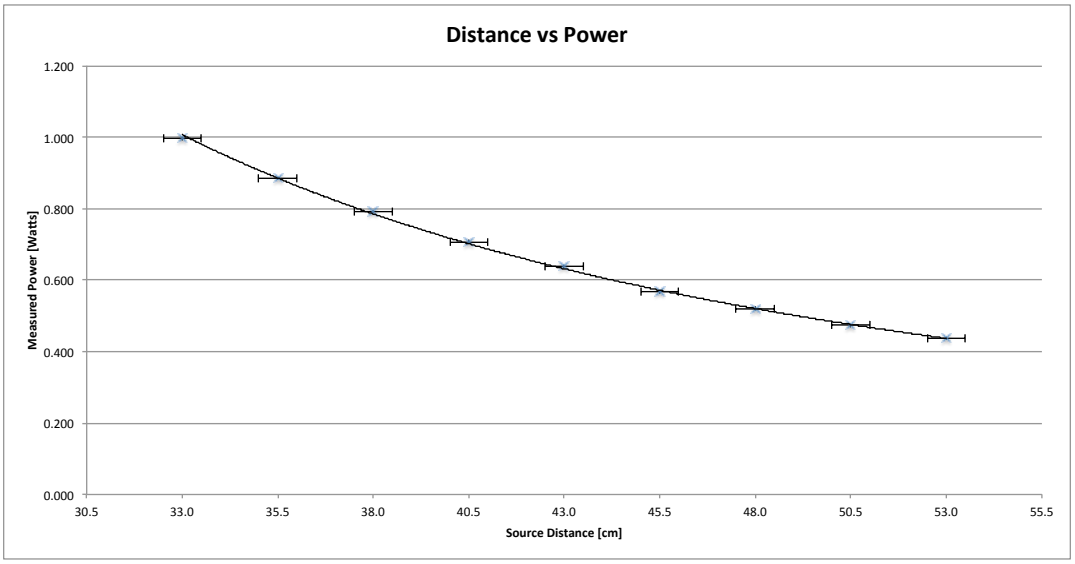

Figure 3.3: A graph to show how the power of the light source changed with distance from the source.

3.3.1 Neutral Density Filters

Neutral density filters (ND filters) reduce intensity across all wavelengths equally. Each ND filter has an optical density value associated with it. The following relationship can be used to calculate the percentage optical transmission thought an ND filter with a given optical density:

$$\text{Optical density} = log_{10}\left(\frac{1}{\text{Transmission}}\right) \tag{3.1}$$

For example, an ND1 filter has an optical density of 1 and a transmission value of 10%. These were the most useful filters for producing Tyndall figures with varying morphology.

3.3.2 RG850 Filter

An RG850 filter cuts all light with wavelength below $850nm$ and transmits all light with $\lambda > 850nm$. This was used to qualitatively test whether infrared radiation could produce Tyndall figures. Imaging is difficult with an RG850 filter because (essentially) all visible light is filtered out, however you can inspect the sample of ice by eye and see whether Tyndall figures have formed. Figure 3.4 shows the transmittance of an RG850 filter [15].

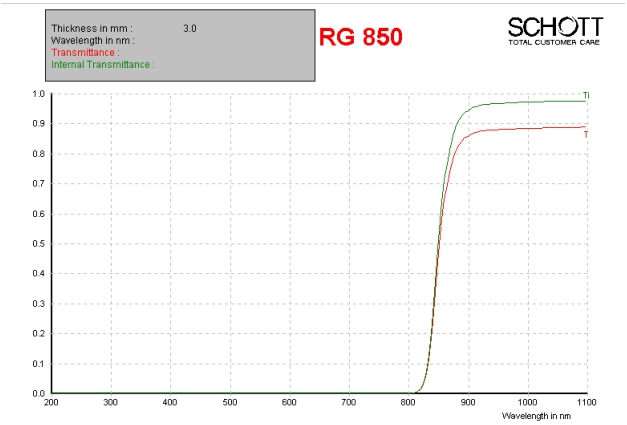

Figure 3.4: A graph to show the transmittance profile of an RG850 filter.

3.3.3 KG1 Filter

A KG1 filter will filter out light in the infrared spectrum but allow visible light to pass. For a halogen source this approximately corresponds to an 80% reduction in power measured. Figure 3.5 shows the transmittance of a KG1 filter [14].

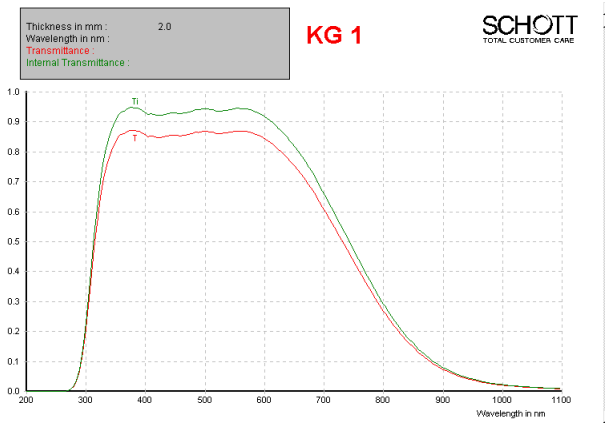

Figure 3.5: A graph to show the transmittance profile of a KG1 filter.

3.4 Imaging System

Because ice is transparent and Tyndall figures are transparent it is difficult to image the figures directly. Placing the camera directly behind the sample of ice being irradiated is difficult because the halogen light source is incredibly bright. Even with the lowest aperture and ISO settings available, the image that the camera captures is too bright to use.

It turns out that the best method for imaging the Tyndall figures is to 'project' the image onto a screen. It is helpful to think of the following imaging set up as being an expanded slide projector. The halogen bulb is the light source, the sample of ice being irradiated is

the 'slide' and the focussing lens from the slide projector is used to focus the image onto a screen. The focussing lens is a HEIDOSMAT converging lens with a focal length of 85mm and a diameter of 28mm. The distance from source to ice is roughly 50cm, with the distance between ice and the focussing lens being 85mm. The focussing lens is mounted on a lens stand and this is mounted on a sliding track. The sliding track enables the lens to be moved closer or further away from the ice, corresponding to the image formed being focussed on a different depth within the sample. By moving the lens on this line, it is possible to 'scan' through the entire sample of ice, from surface to surface.

This is an important limitation to the experimental set up; you can only image Tyndall figures that are in focus. Even if you focus on the centre of the sample, there are large sections that will be completely out of focus. Because the Tyndall figures are transparent, it is difficult to see them unless the water-ice interface happens to be in focus. This makes it very hard to catch the nucleation of Tyndall figures unless you happen to be focussing on the plane that they form in.

In the image on the screen, the water/ice interface appears a dark grey, with the water inside the figure and ice around the outside both appearing as light greys. This suggests that light is diffracted by curvature caused by the third dimensional growth in the direction of the c-axis.

A camera is then used to capture time lapse footage of the projection. The camera used is a Nikon D7000 fitted with a 18-105mm f/3.5-5.6 telescopic lens. This is attached to a pedestal and bolted to the optical bread board, so that the lens is as close to parallel with the focusing lens as possible. The distance from the camera to the screen is roughly 1.5m. I found the optimum settings for taking photographs of the screen to be:

Aperture: F/6.3
Shutter Speed: 1/125s
Exposure Compensation: 0EV
ISO: 160 (but you can set this to auto-metering mode)

The camera should be changed to manual focus mode as the auto focus feature interferes with the time lapse shot spacing. Manually focus the camera onto the screen. This is achieved by placing a plate etched with 5mm squares into the ice holder, focussing the squares onto the screen using the focussing lens, and then focussing the camera onto that image.

The camera can then be connected to the computer via a USB cable. The computer will register that the camera is connected and open a programme called 'Camera Control Pro'. You can use this programme to take time lapse images of the Tyndall figures. All of the camera options can also be changed remotely using this programme.

It is important to implement a sensible protocol for naming the folders that each time-lapse sequence will be saved in. I chose to name one folder for each date that I conducted experiments, in the form YYYY_MM_DD, and then a series of subfolders named 'Test S.N' where S was a number corresponding to the sample of ice that I used and N was the number of the test on that sample. As an example, 'Test 1.2' would correspond to the second test on the first sample of ice for the date that it is saved under. Camera Control Pro is linked

with a programme called ViewNX 2, which is a programme to view photographs in. It will usually start up when you take an image, and will generally display the last image that you captured. As a programme it is useful for navigating through archives of photographs and displaying them full screen.

3.5 Taking Measurements

As well as the images, it is important to note down any observations that you make whilst setting up and conducting the experiment. I have listed some examples of data that I thought it was important to capture below:

1. Pixel Size: The area that a pixel represents. This is measured by placing a transparent piece of acrylic etched with 5mm squares into the ice holder and then taking a picture of the squares as the appear on the screen. By counting how many pixels there are along each 5mm length and averaging, you get a value to convert between pixels and meters. I measured that 1 pixel $= 5 \times 10^{-}6$ Meter square.
2. Power of Light: This is measured using an OPHIR power meter with a P.C.K thermocouple sensor. You cannot measure the power during the experiment as it would obstruct the imaging process. I measured the power after each experiment by fixing the ice holder in place, removing the ice and placing the sensor in the frame.
3. Depth of Tyndall figure in ice: This can be measured by taking advantage of the fact that you can scan through the sample of ice. Once a Tyndall figure has been formed and focussed upon, the focussing lens can be fixed in that position. Once the experiment is over, the ice sample can be removed and a device to measure the depth can be inserted. This device consists of ten, 1mm thick, layers of transparent polycarbonate. Into the surface of each of the these layers is etched a number corresponding to the distance to that layer from the surface. These numbers are arranged in the style of a clock face, and when the device is inserted into the ice holder, one of the numbers will be in focus. It is this number that corresponds roughly to the depth of the Tyndall figure in the ice.
4. General Observations: It is good to note down which filters were used, how thick the sample of ice was, a brief description of the Tyndall figures formed and any other observations that you might have. This will be useful when you come to analyse the images.

I compiled all of these observations into a spreadsheet with an entry for each test that I ran. This catalogue was useful for identifying which results needed to be analysed further.

3.6 Creating and Exporting Movies

As previously mentioned, all time lapse images were saved using a sensible nomenclature and observations were recorded in an excel spreadsheet. It is useful to use MATLAB to analyse

the images and compile them into movies. I found it easiest to convert from time=lapse images to movies using a combination of MATLAB and Quicktime Pro. MATLAB is used to import the images, crop them to display areas of interest and then save each frame as a frame in a .GIF stack. The code to do this is below:

```
%% PREPARE VARIABLES

% Define a variable that holds the frames per second your "movie" should have
gif_fps = 4;
% Define string variable that holds the filename of your gif
video_filename = 'name.gif';

%% FIND IMAGES
%Find image files in folder /IMAGES and assign to variable imageNames
imageNames = dir(fullfile('/Users/Pete/Desktop/Physics/TYNDALL
    FIGURES/Pictures/','Discoid/*.jpg'));
%Convert to a cell array
imageNames = {imageNames.name}';

%% SORT INTO NUMERICAL ORDER
%Images are returned in the order that they are listed in folder. Need to
%be sorted into numerical order
imageStrings = regexp([imageNames{:}],'(\d*)','match');
imageNumbers = str2double(imageStrings);
[~,sortedIndices] = sort(imageNumbers);
sortedImageNames = imageNames(sortedIndices);

rect = [1985 1154 918 918]; %Rectangle is [xmin ymin width height] of crop. This
    particular rectangle corresponds to a 5mm box

%% PROCESS IMAGES USING FOR LOOP

for ii = 1:length(sortedImageNames)
    img = imread(fullfile('/Users/Pete/Desktop/Physics/TYNDALL
        FIGURES/Pictures/','Discoid',sortedImageNames{ii}));

        % crop
        img = imcrop(img,rect); %crops each image using the co-ordinates obtained
            above

        % convert to indexed image for gif format
        [imind,cm] = rgb2ind(img,256);
        % If first loop iteration: Create the file, else append to it
        if ii == 1;
           imwrite(imind,cm,video_filename,'gif', 'Loopcount',inf);
        else
            imwrite(imind,cm,video_filename,'gif','WriteMode','append','DelayTime',1/gif_fps);
        end

end
```

In order for this to work, images in each folder should be saved as numbers i.e. 'Image 1' should be called '001.jpg', 'Image 2' called '002.jpg' etc. You can use a bulk renaming programme to do this, or automate a process using 'automator.app' if you are using a mac. You could probably get MATLAB to rename the files but I did not pursue this.

This code will produce a .gif file, which is a stack of all of your images. You can then use Quicktime Pro to compile this gifstack into a movie format.

3.7 Image Analysis

It would be useful to know the area and perimeter of an imaged Tyndall figure, as these would allow measurement of the growth of the figure. I began a MATLAB code to measure this. It appears that the best way to produce an image processing code is to create a code that works for one image and then wrap it in a for loop when you want to apply it to many images. The code I began is below:

```
% load image and convert to grayscale
tyrgb = imread('TyndallTest.jpg');
ty    = rgb2gray(tyrgb);
figure; imshow(ty)

% apply a weiner filter to remove noise.
% N is a measure of the window size for detecting coherent features
N=20;
tywf  = wiener2(ty,[N,N]);
tywf = tywf(N:end-N,N:end-N);

% rescale the image adaptively to enhance contrast without enhancing noise
tywfb = adapthisteq(tywf);

tyedb = edge(tywfb,'sobel',0.012);

%join edges
%uses a structural morphological transformation to join the edges
diskEnt1 = strel('disk',7); % radius of 7
tyjoin1 = imclose(tyedb,diskEnt1);

% interactively fill internal regions
%click on regions to fill
[ny nx] = size(tyjoin1);
figure; imshow(tyjoin1)
tyjoin2=tyjoin1;
titl = sprintf('click on a region to fill\nclick outside window to stop...')
while 1
   pts=ginput(1)
   tyjoin2 = bwfill(tyjoin2,pts(1,1),pts(1,2),8);
   imshow(tyjoin2)
   title(titl)
   if (pts(1,1)<1 | pts(1,1)>nx | pts(1,2)<1 | pts(1,2)>ny), break, end
end
```

It should then be possible to use the `regionprops` command in MATLAB to measure this, however due to time constraints I did not manage to make this work. Below is a code that works for finding the area of white circle on a black background:

```
%% Read in RGB image from directory
RGB1 = imread('1.jpg') ;

%% Convert RPG image to grayscale image
I1 = rgb2gray(RGB1)     ;

%% Transform Image
%CROP
IC1 = imcrop(I1,[74 43 278 285]); %Rectangle is [xmin ymin width height] of crop.

%BINARY IMAGE
BW1 = im2bw(IC1); %Convert to binary image so the boundary can be traced

%DRAW PERIMETER
BWP1 = bwperim(BW1);
%Traces perimeters of objects & colours them white (1).
%Sets all other pixels to black (0)

%FILL PERIMETER WITH WHITE IN ORDER TO MEASURE AREA AND PERIMETER
BWF1 = imfill(BWP1); %This opens figure and allows you to select the areas to fill
    with white.

%MEASURE PERIMETER
D1 = regionprops(BWF1, 'area', 'perimeter');
%Returns an array containing the properties area and perimeter.
%D1(1) returns the perimeter of the box and an area value identical to that
%perimeter? The box must be bounded by a perimeter.
%D1(2) returns the perimeter and area of the section filled in BWF1

%% Display Area and Perimeter data
D1(2)
```

This method should work for Tyndall figures, but the edge detection algorithm struggles to preserve the intricacies of the interface and it is time consuming to fill the image that it produces. If it was possible to programmatically fill the figure then it would be a viable solution. Figure 3.6 shows an example of the edge detection.

Since the wavenumber of the perturbation is important to us, it would be good to find a technique that preserves this detail.

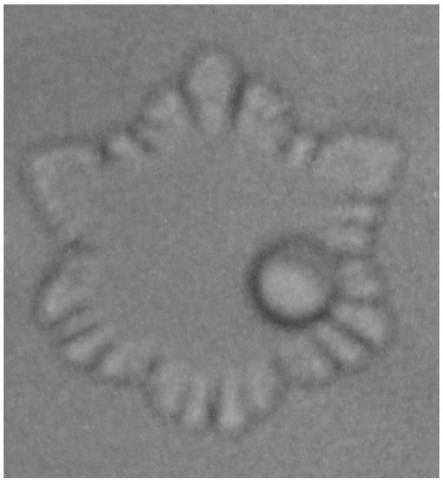

(a) Tyndall figure test image

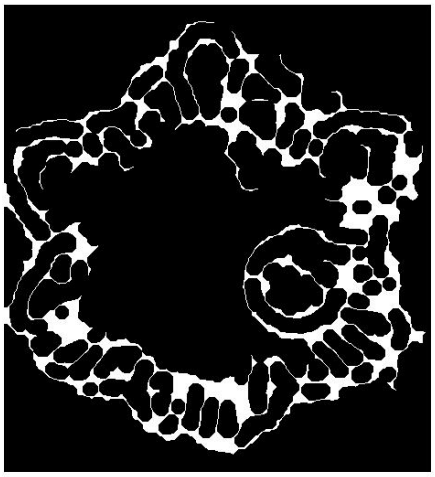

(b) Test image with edge detection applied

Figure 3.6: Tyndall figure before and after edge detection

3.8 The Greedy Snake Algorithm

In my final week I discovered an algorithm called 'The Greedy Snake Algorithm', which is also known as active contours. It works like a lasso or elastic band closing around a shape. A set of initial points surrounds the image and then these points move through an iterative process to advance towards the edge of the shape. There are a variety of sources explaining the greedy snake: this applet is fairly useful at explaining what it does interactively [2], and there is a book that looks like it could be helpful [1]. There is a MATLAB package that contains the algorithm [8]. Again, due to time constraints I did not manage to make this work, but I believe that active contours will be the best way to extract perimeter and area data from the images captured.

I wrote a code to test the algorithm. It manages to close the loop around the test image, but then passes through the outer edge. I am unsure as to why this is the case. The code is below for reference. It uses the MATLAB package mentioned above, which you can download from the MATLAB exchange.

```
% load image and convert to grayscale
tyrgb = imread('TyndallTest.jpg');
ty    = rgb2gray(tyrgb);


% apply a weiner filter to remove noise.
% N is a measure of the window size for detecting coherent features
N=20;
tywf  = wiener2(ty,[N,N]);
tywf = tywf(N:end-N,N:end-N);
```

```
% rescale the image adaptively to enhance contrast without enhancing noise
tywfb = adapthisteq(tywf);

% apply a canny edge detection
tyedb = edge(tywfb,'canny');


%join edges
diskEnt1 = strel('disk',8); % radius of 4
tyjoin1 = imclose(tyedb,diskEnt1);

%invert image
I = imcomplement(tyjoin1);

figure; imshow(I); [y,x] = getpts;

P=[x(:) y(:)];

 % Start Snake Process
   Options=struct;
   Options.Verbose=true;
   Options.Wedge= 3.0;
   Options.Sigma1 = 10;
   Options.Sigma2 = 5;
   Options.Iterations=600;
   [O,J]=Snake2D(I,P,Options);
  % Show the result
   Irgb(:,:,1)=I;
   Irgb(:,:,2)=I;
   Irgb(:,:,3)=J;
   figure; imshow(Irgb,[]);
   hold on; plot([O(:,2);O(1,2)],[O(:,1);O(1,1)]);
```

Chapter 4

Results

A system for producing Tyndall figures has been designed, tested and proved to be effective. Tyndall figures of varying types were produced and imaged.

Qualitatively, a relationship between the morphology of Tyndall figures and the power of light used to irradiate the samples has been established.

At low power (around Power = 0.1810.005 Watts), discoid Tyndall figures were observed to form. The figures imaged were incredibly faint, with it often being impossible to focus on the water-ice interface. This suggests small growth in the c-axis leading to very little diffraction of light at the interface. Growth was observed to be markedly slower than at higher powers and the interface was not observed to go unstable. This suggests little superheating in the ice. Figure 4.1a is an example of this.

For medium values of power (around Power = 0.4370.005 Watts) Tyndall figures were observed to initially form and grow as discoids, before becoming unstable at the interface. The Circular discs were often observed to tend towards a hexagonal shape, which then becomes unstable with a high wavenumber perturbation at the interface. Figure 4.1b is an example of this.

For higher powers of light (around Power = 0.5820.005 Watts) the discoid mode of growth is barely observed at all. It is replaced by dendritic growth with a six-fold symmetry. These Tyndall figures look more like the flowers that Tyndall described in his initial observations. Figure 4.1c is an example of this.

At even higher powers of light, Tyndall figures were observed to form and grow with a highly dendritic regime. Figure 4.1d is an example of this.

A complete catalogue of the images taken over the summer is in a separate document as they were recorded in a Microsoft Excel spreadsheet.

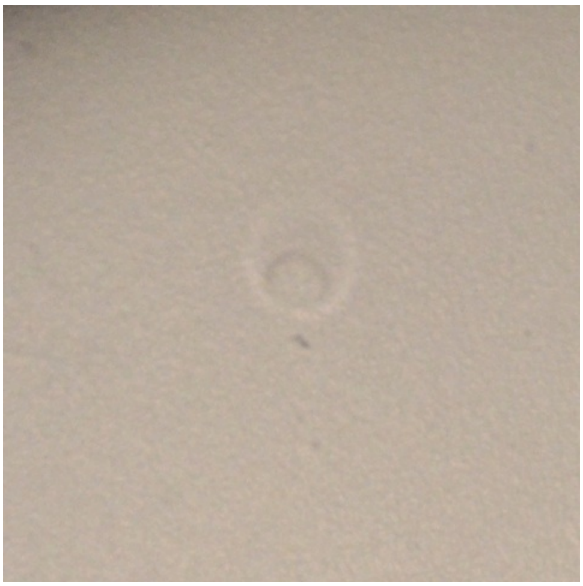

(a) Faint Discoid Tyndall Figure

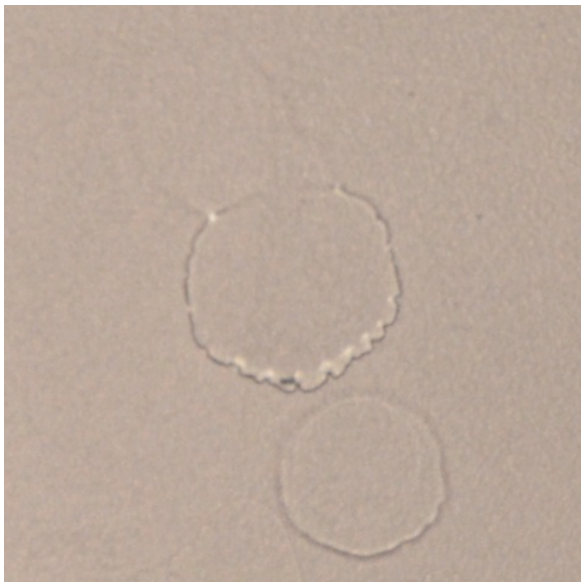

(b) Unstable Discoid Tyndall Figure

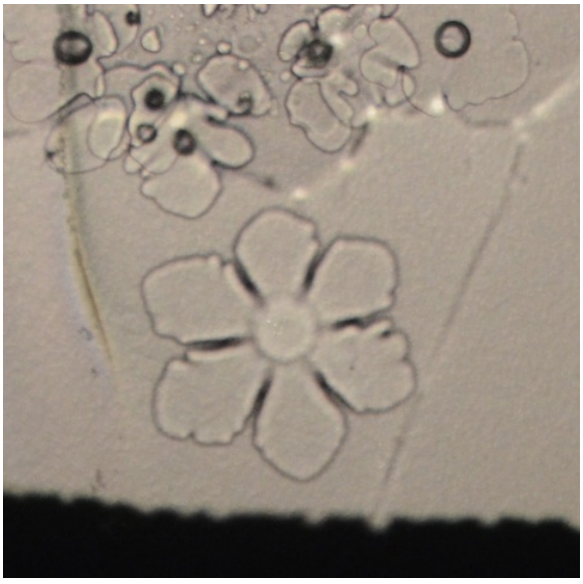

(c) Flower Tyndall Figure

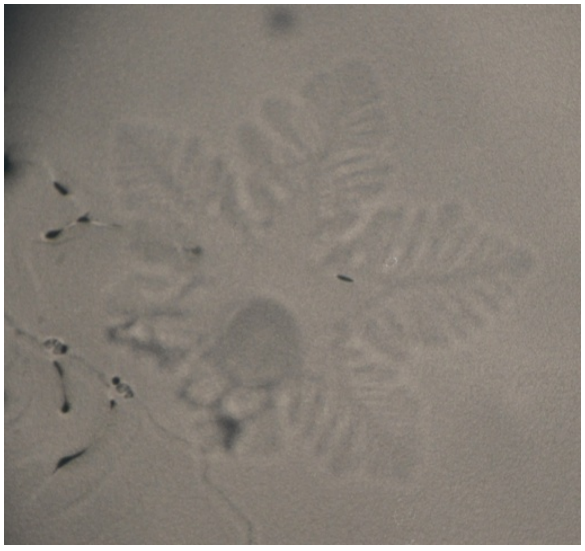

(d) Dendritic Tyndall Figure

Figure 4.1: Examples of Tyndall figures formed in the Lab

Chapter 5

Attempts at Forcing Nucleation of Tyndall Figures

The main limitation on the number of experiments that yielded good time-lapse image sequences was that Tyndall figures could nucleate anywhere in the sample. Furthermore, on some tests a large number of Tyndall figures with inconsistent morphologies were formed. This leads me to believe that the character of the nucleation point may also have an effect on the morphology of Tyndall figures.

If you could position a nucleation point at a known location within a sample of ice, then you could focus on that point and capture the formation of Tyndall figures from nucleation. If all nucleation points were identical, then the results would be more comparable (and hopefully more consistent). With this in mind, I set about trying to embed a nucleation point in the samples of ice.

The first method I tested was trying to get ice to form over grains of sand. I grew ice single crystals, removed them from the freezer and allowed them to melt for a while. A small layer of water formed on the top of the samples. I placed grains of sand under the surface of the water using tweezers and then placed the sample back in the freezer, hoping that the ice would grow around the sand. In reality the ice grew upwards towards the surface of the water, rejecting the sand. So I was left with a sample of ice with grains of sand lying on the surface. Clearly another technique was required.

I next tried using a heated needle to drill into the samples of ice. To begin with, I used a standard sized clothes pin, heated in a bath of hot water. Once warm, I applied pressure and 'drilled' a hole into the sample of ice. I could then drop a single grain of sand into the hole I had drilled and fill over the grain of sand with distilled water. This was placed back in the fridge to freeze over. Upon irradiation, a large number of Tyndall figures nucleated in concentric circles around the pin hole. It appears that either the heat or the pressure applied to the sample had created damage to the lattice, causing Tyndall figures to nucleate. Figure 5.1 shows an example of the damage caused by the heat drilling. Clearly it would be hard to create a hole in the ice sample without causing to much stress on the lattice.

I encountered the most success when I began using a device to hold the needles vertically,

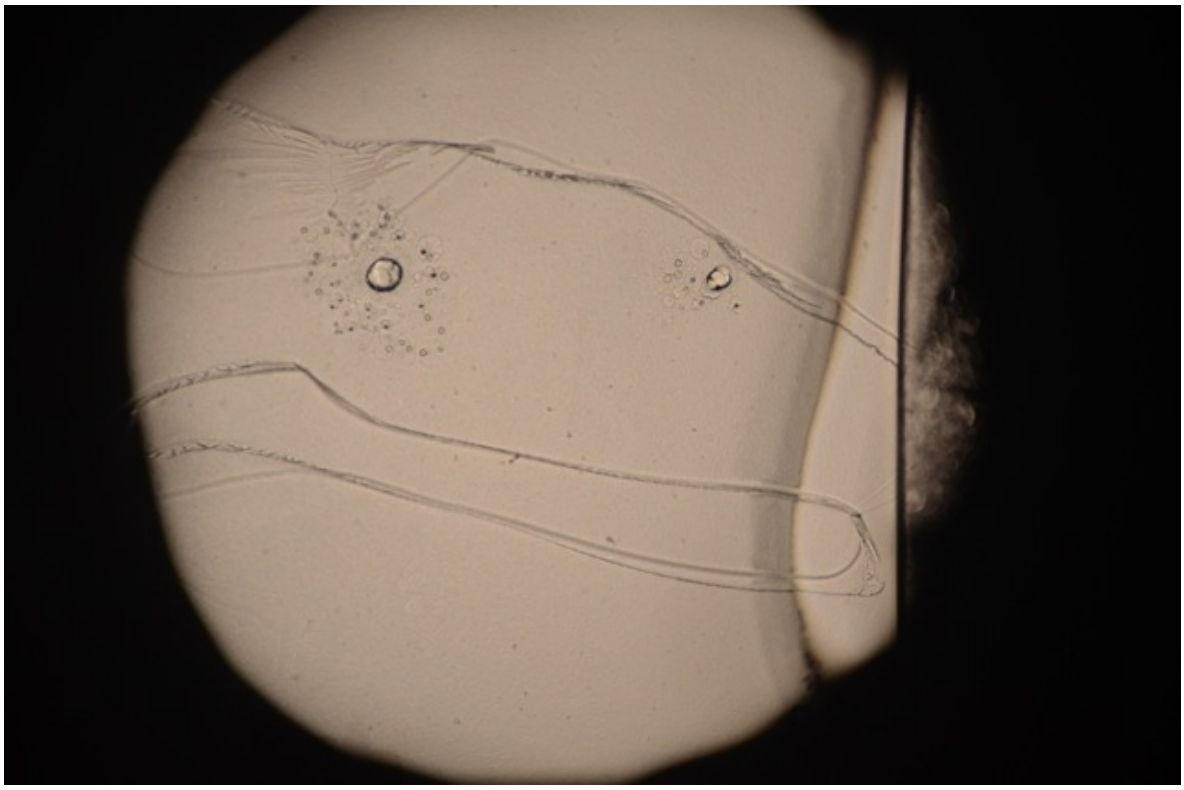

Figure 5.1: Image to show the damage to the ice lattice caused by the heat drilling.

with the tip of the needle around 5mm beneath the surface of the water. I seeded the ice as normal, and it grew around the needles. Once growth was complete it was possible to remove the sample of ice, allow it to warm for a while and then remove the needles. This would leave holes that I could place the sand into and then fill with water and freeze over. This technique stopped the nucleation of Tyndall figures around the hole, but irregular melt figures were nucleated by the sand. Sand is not particularly symmetric, so I wondered if a symmetric nucleation point might produce better results.

I then tried embedding tiny 250μm microspheres by dropping them into the holes left by the ice growing around the needles. The holes were then filled with distilled water and left to freeze over. The microspheres yielded better results than the sand but still did not produce good Tyndall figures. Often the microspheres would nucleate melting at different depths of the surrounding ice, making it hard to focus on one melt figure. Similarly, the ice that formed to fill the hole would melt, causing the microsphere to move and difficulties in focussing on one melt figure.

Sastoshi Takeya managed to produce Tyndall figures from the tip of a 0.05mm Cu-Constantin thermocouple [16], so it should be possible to produce Tyndall figures from an impurity that is placed in the ice crystal. Unfortunately Takeya did not include any pictures of his Tyndall figures in the letter referenced above so there is know way of knowing what form they took.

Chapter 6

Reflection and Suggested Further Work

All of the initial aims of the project were achieved. A system for producing and imaging Tyndall figures has been put in place and a large number of good image sequences were captured. Initially, the overriding limitation on experiments was the number of samples of ice that could be prepared per day. The process for growing ice has been refined and reliably produces three sample of ice per day.

The next step for refining the procedure is to find a way to embed impurities at a known position in the ice crystal. This should lead to every experiment producing good, clear image sequences which will be directly comparable to each other. Investigations into the suitability of 250μm microspheres as points for nucleating Tyndall figures were carried out. More experimentation is required to test the suitability as no conclusive evidence was found to state whether they are suitable (or not). Attempting to reproduce Takeya's [16] experiments could be a good first step, although it would be difficult to know how successfully his method had been duplicated without images of the Tyndall figures that he formed.

With regards to the analysis of the image sequences, simple methods for finding the edges of Tyndall figures using MATLAB have been explored. I believe that the greedy snakes algorithm shows the most promise for the analysis required to find the rate of growth of Tyndall figures. Further development of these image processing techniques would be worthwhile, as knowing the rate of growth would enable comparison with the mathematical models that are being worked on.

Bibliography

[1] M. Isard A. Blake. *Active Contours: The Application of Techniques from Graphics, Vision, Control Theory and Statistics to Visual Tracking of Shapes in Motion*. Springer.

[2] Electronics and Univ Southampton Computer Science. Active contours and snakes, August 2013.

[3] N. Riehl H. Engelhardt, B. Bullemer. Protonic conduction of ice part ii: Low temperature region. *Physics of Ice*, 1969.

[4] Matthew Hennessy. Liquid snowflake formation in superheated ice. Master's thesis, St Hugh's College, Univ. Oxford.

[5] A. Higashi. Growth and perfection of ice crystals. *Journal of Crystal Growth*, 1974.

[6] Peter V. Hobbs. *Ice Physics*. Oxford University Press.

[7] C. A. Knight. A simple technique for growing large, optically "perfect" ice crystals. *Journal of Glaciology*, 1996.

[8] Dirk-Jan Kroon. Snake: Active contour, August 2013.

[9] J. S. Langer. Instabilities and pattern formation in crystal growth. *Reviews of Modern Physics*, 1980.

[10] S. Magun M. Kass. Zur uberhitzung am phasenubergang fest-flussig. *Z. Kristallogr*, 1961.

[11] N. Maeno. Nuclei of tyndall figures and surface melting of ice. *Canadian Journal of Physics*, 1968.

[12] U. Nakaya. Properties of single crystals of ice, revealed by internal melting. *Snow, Ice and Permafrost Research Establishment*, 1956.

[13] D. V. D. Roos. Rapid production of single crystals of ice. *Journal of Glaciology*, 1975.

[14] Schott. Kg1 data sheet, August 2013.

[15] Schott. Rg850 data sheet, August 2013.

[16] S. Takeya. Growth of internal melt figures in superheated ice. *Applied Physics Letters*, 2006.

[17] J. Tyndall. On some physical properties of ice. *Philosophical Transactions of the Royal Society of London*, 1958.

[18] Zeiss. Tungsten-halogen incandescent lamps, August 2013.